Scientific Research Publishing

Journal of Minerals and Materials Characterization and Engineering, 2025, 13(5), 292-304
https://www.scirp.org/journal/jmmce
ISSN Online: 2327-4085
ISSN Print: 2327-4077

Physico-Chemical and Geotechnical Characterization of Two Clays from the Town of Dabou (Youhouill) with a View to Their Industrial Recovery

Wilfried Aristide Atsé, Marc Marie-Maurice Mélèdge Essi

Laboratoire de Constitution et Réaction de la Matière, Université Félix Houphouët Boigny, Abidjan, Côte d'Ivoire
Email: wilfriedaatse@gmail.com

How to cite this paper: Atsé, W.A. and. Essi, M.M.M.M. (2025) Physico-Chemical and Geotechnical Characterization of Two Clays from the Town of Dabou (Youhouill) with a View to Their Industrial Recovery. *Journal of Minerals and Materials Characterization and Engineering*, **13**, 292-304.
https://doi.org/10.4236/jmmce.2025.135016

Received: June 17, 2025
Accepted: September 23, 2025
Published: September 26, 2025

Abstract

This study focuses on the characterization of two clays from Dabou (southern Côte d'Ivoire) for their potential industrial use. The study analyses two clay samples (DAB1, DAB2) from southern Cote d'Ivoire using X-ray Diffraction (XRD), Inductively Coupled Plasma Atomic Emission Spectroscopy (ICP-AES), Energy Dispersive X-ray Spectroscopy (EDS) mapping, laser/sedimentation granulometry and Atterberg limits. We analyzed samples to determine their mineralogical, chemical, physical and geotechnical composition. The results reveal a predominance of kaolinite, quartz, goethite and illite. Silica and alumina contents are appropriate for use in ceramics. Both clays are kaolinite-rich aluminosilicates with elevated Fe_2O_3. Physical properties such as plasticity and grain size confirm their suitability for brick and tile production, while the iron content suggests possible application as heterogeneous Fenton catalysts for dye-laden wastewater. They are also suitable for other ceramic products and the iron content of these samples is high. These results emphasize the potential for local use of these clays in the building and craft industries. They can also serve as catalytic support for the Fenton process to treat dye-rich water.

Keywords

Dabou Clays, Ivory Coast, Kaolinite, Ceramics, Characterization

1. Introduction

Clays represent important natural materials in many sectors including ceramics, civil engineering, environmental applications, and pharmacology. Geological investigations conducted between 1963 and 1969 by the Société de Développe-

ment Minier (SODEMI) revealed that Côte d'Ivoire has many deposits of clay materials [1]. Regardless of their abundance these significant resources remain considerably unexploited. The understanding of the geotechnical behavior of fine soils particularly clays, is a central condition for the design and construction of civil engineering infrastructure [2]. In humid tropical areas like the south of Côte d'Ivoire, the characteristics of clay soils are impacted by climatic conditions, the geological composition of the natural bedrock, and the pedogenetic processes [3]. These factors directly affect their physical and mechanical properties, thereby determining their performance under loading conditions and their stability [4]. The objective of this study is to examine the geotechnical properties of two clays that are collected from the southern region of Côte d'Ivoire using granulometric analysis, porosity tests, and Atterberg limit tests. These parameters enable the evaluation of soil plasticity, consistency, and the textural characteristics [5]. And provide essential data for soil classification and their suitability for diverse types of structures. The purpose is to increase the understanding of regional soils and provide valuable data for infrastructure development and building projects [6].

2. Materials and Methods

2.1. Study Area

Two clays named DAB1 and DAB2 were collected in the town of Dabou. The samples came from the village of Youhouill in the Grand Pont region of southern Côte d'Ivoire. The clay sampling site is located at geographic coordinates 05˚21'29"N and 04˚3'18"W.

2.2. Sampling

We collected clay samples on site using a hoe. We placed the samples in 25 kg nylon bags. We then transported them to the laboratory. For each sample, we took 5 bags of 25 kg from each site.

2.3. Sample Preparation

Before characterization, we dried samples in the shade for three days. We crushed, crumbled, washed and dried the clay blocks. We ground a portion of each sample in a glass mortar. We sieved the powder through a 100 µm sieve to obtain a homogeneous powder for analysis.

2.4. Mineralogical Analysis

We weighed 2g of clay and ground it in an agate mortar. We sieved the rock powder through a 63µm sieve. We placed the collected powder in the sample holder and compacted it with a glass plate. We then analyzed it by XRD. The analysis parameters were 28 mA current, 20 kV voltage, 1 kW power and 4.5 mA filament amperage. The monochromatic radiation for the measurements was the copper Kα line (λ = 1.5406 Å). The sample holder was tilted at an angle of 4˚. We per-

formed phase identification with Match software. We used the GBC-EMMA diffractometer for X-ray diffraction.

2.5. Chemical Analysis

We determined the chemical composition of the clays by ICP-AES and EDS X-ray mapping. We carried out chemical analysis by ICP-AES with an ANTON Paar spectrometer. Before measurement, we put samples into a solution using a microwave-assisted chemical process. The procedure involved several steps. We introduced 30 mg of each sample with a particle size of 100 µm or less into a Teflon tube. We had previously dried the samples at 110˚C for 24 hours. We added 4 mL HF (28 vol%) and 1 mL HNO_3 (68 vol%) to the tube. We placed the assembly into a microwave device (CEM, MARS 5) and subjected it to a 45-minute cycle. Dissolution took place during a 20-minute rise in temperature (Tmax = 180˚C) and pressure (pressure reached = 3 MPa). This was followed by a 20-minute plateau at 180˚C. We then cooled the sample to room temperature. After dissolution, we made up the volume to 250 ml in a volumetric flask for analysis. We acquired X-ray mapping over the entire sample surface with an X FLASH 6/30 EDS spectrometer. We suspended a small mass of the sample in ethanol and ultrasonicated it for five minutes. We then pipetted a drop onto a polished sample holder. We placed the sample holder in a box and dried it in ambient laboratory air. Finally, we put it under the microscope for energy dispersive analysis.

2.6. Geotechnical Analysis

We carried out granulometric analysis on dried clay samples with laser granulometry. We used PARTICA HORIBA equipment for this analysis. We performed granular analysis by sedimentation on dried clay samples that were crushed and sieved to 100 µm. We conducted particle size analysis by sieving and sedimentometry according to standards NF P18-560 [7] and NF P94-057 [8] respectively. We determined the liquidity limit (WL) using the Casagrande disk method. We determined the plasticity limit (WP) using the roller method. We determined these Atterberg limits according to standard NF P94-051 [9].

3. Results and Discussion

We have already published the results of x-ray diffraction and ICP-AES chemical analysis. This article presents the continuation of previous work [10]. The drying process is conducted at low temperatures, and its duration can vary from several hours to several days depending on factors such as the product's morphology, the raw materials used, and particle size distribution [11] [12]. These parameters significantly influence the rate and efficiency of moisture removal during drying [13]. Porous pottery made from very melting clays can be fired at around 850˚C. However, some aluminous porcelains require firing at over 1450˚C. Refractory clays (Al_2O_3 greater than 35%); clays for terracotta (bricks, tiles, earthenware): TiO_2 + Fe_2O_3 greater than 3% [14]. Given the results of the ICP-AES [10], our samples

could be used in terracotta (bricks, tiles, earthenware).

3.1. Mineralogical Results (XRD)

We reported elsewhere [10] that x-ray diffraction analysis revealed the composition of the DAB1 and DAB2 clay samples. These samples consist mainly of kaolinite, goethite, illite and quartz [10]. [15] made aquatic filters according to the formulation "clay stabilized at 4% of cement mixed with 4% of kambala sawdust and 10% of white sand" then heated to 1050˚C to decontaminate the waters of gutters and wells. The authors carried out geotechnical, geochemical, thermal, infrared spectroscopy, and scanning electron microscopy to analyze the clay material. Also, some researchers [16]-[23] have used clays in industrial fields (brick making, environment). The authors obtained characterization results similar to ours.

3.2. Chemical Results (ICP-AES)

We carried out chemical analysis on samples DAB1 and DAB2. The results show significant quantities of silica SiO_2 at 67.54% for DAB1 and 58.21% for DAB2. Alumina Al_2O_3 content reached 21.87% for DAB1 and 28.11% for DAB2. Sample DAB1 contains more silica than sample DAB2. However, DAB1 contains less alumina Al_2O_3, iron oxide Fe_2O_3, potassium oxide K_2O and titanium oxide TiO_2 than sample DAB2. The Fe_2O_3 iron oxide content is relatively high in both samples. K_2O, Na_2O and TiO_2 oxides appear in small quantities [10]. Chemical analyses revealed high levels of silica (SiO_2: 58% - 68%) and alumina (Al_2O_3: 21% - 29%). These levels characterize alumino-silicate clays. Iron (Fe_2O_3: 8% - 12%) is also present. We calculated the Al_2O_3/Fe_2O_3 ratio as 2.44 for DAB1 and 2.43 for DAB2. Both ratios fall below 5.5. These samples are therefore rich in iron. They can be manufactured into building materials such as bricks and tiles [16]-[18] [24]. ICP-AES (Inductively Coupled Plasma Atomic Emission Spectroscopy) offers a more precise and quantitative assessment of elemental compositions compared to EDS (Energy Dispersive X-ray Spectroscopy), which provides semi-quantitative results.

3.3. Chemical Mapping of Samples DAB1 and DAB2

Figure 1 shows chemical mapping of sample DAB1. Technical limitations prevented us from conducting chemical mapping of sample DAB2. Aluminum and Oxygen distribute homogeneously throughout the sample. Carbon, Silicon, Iron and Titanium concentrate in specific areas while maintaining equal distribution throughout the sample. These chemical elements are therefore superimposable. Carbon (in red) originates from organic matter present in the soil's natural environment. This analysis did not identify Potassium and sodium. The chemical mapping study reveals that DAB1 clay consists essentially of C, O, Al, Si, Fe and Ti. This composition aligns with the different phases detected during mineralogical characterization of these clays. The phases include $Si_2O_5Al_2(OH)_4$ for kaolinite,

FeO(OH) for goethite and SiO_2 for quartz.

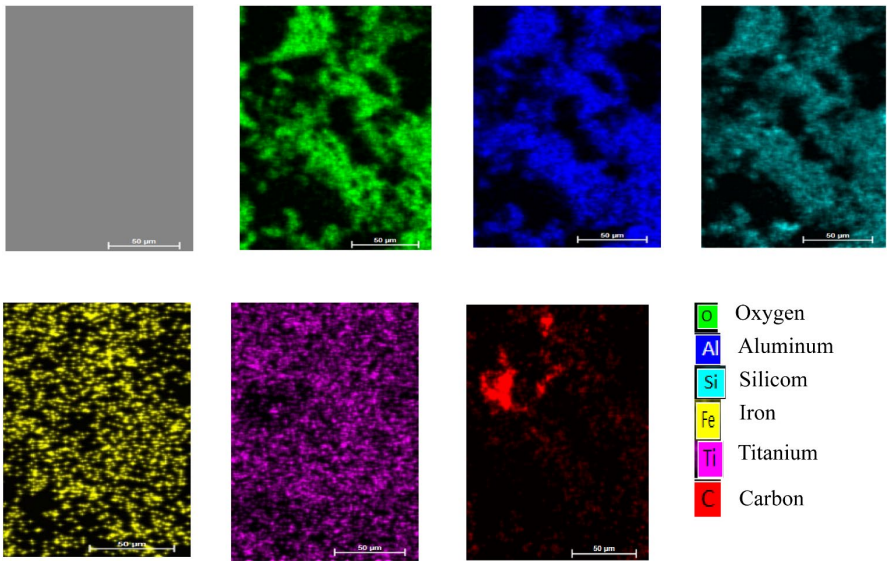

Figure 1. Chemical mapping of DAB1.

3.4. EDS spectra of samples DAB1 and DAB2

EDS analysis is a semi-quantitative analysis. EDS analysis allows the identification and quantification of the elements present, as well as the visualization of their spatial distribution within the sample by detecting the X-rays emitted when it is bombarded by an electron beam. **Figure 2** and **Figure 3** show the EDS spectra of samples DAB1 and DAB2. This analysis did not identify potassium and sodium. However, ICP-AES chemical composition analysis identified these two chemical elements in oxide formation at low percentage rates. The silica and alumina contents indicate that these two samples are aluminosilicates. The iron content could induce the production of hydroxyl radicals via the Fenton reaction. The low potassium oxide content could suggest the presence of illite and muscovite. Carbon relates to contamination and originates from organic matter present in the clay's natural environment. The presence and concentration of oxygen may indicate formation of various oxides or oxygenated compounds. These compounds are essential for understanding the material's properties. High oxygen levels in geological studies can indicate weathering processes. These processes transform primary minerals into more oxygen-rich secondary minerals such as clays. The much higher iron levels in these samples are responsible for their brick-red color. This vibrant hue is a real advantage, as it can be used as a natural colorant for clay bricks and tiles [18] [24]. Iron in clay raw materials can be "structural", *i.e.*, it replaces Si^{4+} or Al^{3+} cations in tetrahedral and/or octahedral layers. It can also be "non-structural", occurring as individual particles such as oxyhydroxides, e.g, goethite (α-FeOOH) and lepidocrocite (γ-FeOOH), or as oxides such as hematite (α-Fe_2O_3) and maghemite (γ-Fe_2O_3) [25] [26].

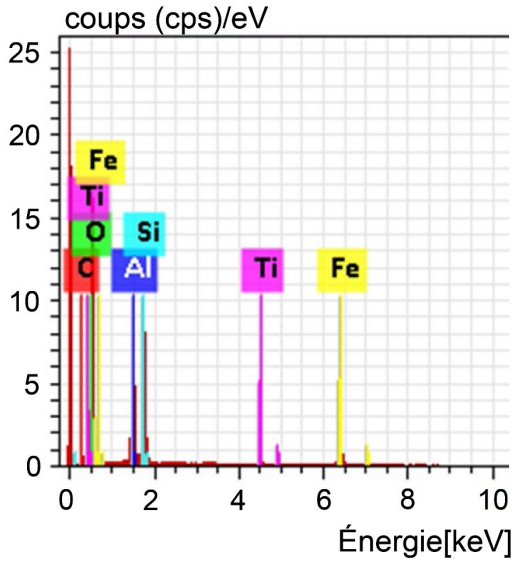

Figure 2. EDS spectrum of DAB1.

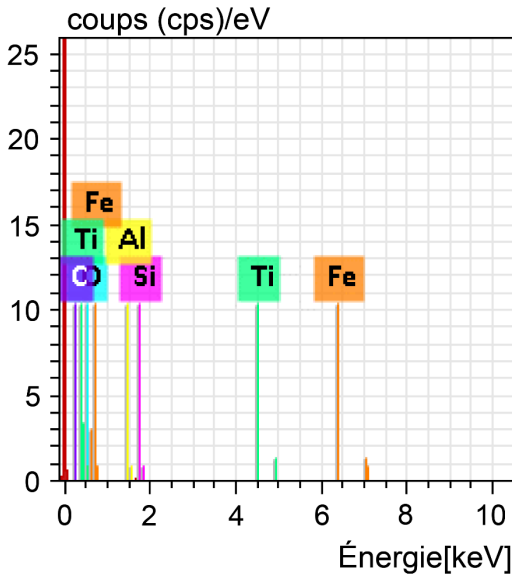

Figure 3. EDS spectrum of DAB2.

We present microanalysis of samples DAB1 and DAB2 by EDS (mass%) in Table 1. Quantification by microanalysis shows the composition of both samples. Sample DAB1 contains 11.92% carbon (C), 49.41% oxygen (O), 12.93% aluminum (Al), 15.74% silica (Si), 0.84% titanium (Ti) and 9.22% iron (Fe). Sample DAB2 contains 11.33% carbon (C), 78.96% oxygen (O), 12.42% aluminum (Al), 14.74% silica (Si), 0.79% titanium (Ti) and 7.65% iron (Fe). These results are similar to those of other authors with different composition percentages [27]-[29].

3.5. Particle Size Analysis by Laser Diffraction

Laser diffraction and sedimentation (sedimentometry) are two widely employed methods for analyzing particle size distributions in materials such as soils, clays,

and suspensions. Despite their common application, these techniques rely on distinct physical principles, which can occasionally produce discrepant or complementary results in the characterization process. Granulometric analysis was performed through sedimentation on dried, crushed, and 100 µm-sieved clay samples. Particles exceeding 2 mm in diameter were removed using a 2 mm (10 mesh sieve). The sieved material was homogenized, and approximately 40 g of the dried sample was dispersed in water containing a dispersing agent before being transferred into a graduated cylinder. The mixture's density was then measured at various time intervals, ranging from 30 seconds to 24 hours, using an oedometer. Monitoring the variation in density over sedimentation time enabled the determination of the particle size distribution within the sample. Prior to detailed characterization, the samples were sieved with a 100 µm mesh. Traditionally, sieving is used to separate coarse particles larger than 40 µm, while laser diffraction techniques are typically applied to analyze finer powders in the micrometer range. Particle size distribution is derived from the interaction between incident radiation and individual particles, allowing for accurate measurement of grain sizes spanning from a few micrometers up to several millimeters in particulate samples. The results of the laser diffraction particle size analysis are presented in Table 2. The various mean diameters, namely d_{10}, d_{50}, and d_{90}-correspond to the particle volumes below which 10%, 50%, and 90% of the total volume are contained, respectively. These data indicate that the DAB1 clay exhibits a finer particle size distribution compared to DAB2. The higher values of d50 and d90 observed in DAB2 suggest the presence of significant particle agglomeration, likely resulting from inadequate dispersion of the suspension [30].

Table 1. EDS Microanalysis of samples DAB1 and DAB2 expressed in % by mass.

Chemical element	DAB1	DAB2
Carbon	11.92	9.00
Oxygen	49.41	62.71
Aluminum	12.93	9.87
Silicon	15.74	11.71
Titanium	0.84	0.63
Iron	9.16	6.08
Total	100.00	100.00

Table 2. Particle size distribution.

Samples	d_{10} (µm)	d_{50} (µm)	d_{90} (µm)
DAB1	6.16	11.16	81.39
DAB2	27.77	47.71	87.11

3.6. Particle Size Analysis by Sedimentometry

Table 3 presents the sedimentometric particle size distribution for the clay samples DAB1 and DAB2. The analysis indicates that DAB1 comprises approximately 47.8% silt and 52.2% clay, while DAB2 consists of about 47.5% silt and 52.5% clay. These results demonstrate that both samples have comparable proportions of silt and clay fractions.

Table 3. Mechanical and sedimentometric particle size analysis of DAB1 and DAB2.

Proportions	]63 µm - 32 µm]	]32 µm - 16 µm]	]16 µm – 8 µm]	]8 µm – 4 µm]	<4 µm	Total	To Moyenne
DAB1	40.1	1.7	3.7	2.3	52.2	100	4.83
DAB2	38	1.7	2.2	5.6	52.5	100	4.98

3.7. Atterberg Limits

Atterberg limits are fundamental parameters used to characterize the consistency and plasticity of fine-grained soils, with their values being influenced by particle size distribution and mineralogical composition. Determining these limits is a standard method for evaluating the mechanical behavior of clays [31], as they reflect changes in soil behavior relative to water content. The liquid limit (W_L) marks the transition of a soil from a plastic to a liquid state, indicating the minimum water content at which the soil becomes flowable. Conversely, the plastic limit (W_P) defines the boundary between plastic and solid states and corresponds to the maximum water content at which the soil can be deformed without crumbling. The difference between these two limits, known as the plasticity index (I_P), provides valuable insights into soil plasticity. For the samples studied, the plasticity indices were 37 for DAB1 and 30 for DAB2. According to [32], soils with I_P values between 20 and 40 are classified as plastic, indicating that both DAB1 and DAB2 are indeed plastic clays. We present these results in Table 4. The W_L liquidity limit values are 72% for sample DAB1 and 58% for sample DAB2. Samples DAB1 and DAB2 show W_P plasticity limits of 35% for DAB1 and 28% for DAB2. The plasticity index values are 37 for DAB1 and 30 for DAB2. The consistency index Ic shows little variation. The value for DAB2 (1.99) is higher than that for DAB1 (1.88). The average Ic of 1.93 for both clay samples is greater than 1.

3.8. Specific Surfaces, Densities and Porosities of Samples DAB1 and DAB2

The specific surface area expressed ($m^2\ g^{-1}$) represents the total surface area of particles per unit mass. It is highly dependent on particle size. Density depends on particle arrangement and porosity. Porosity is the ratio of void volume to total soil volume. It is directly dependent on particle size distribution. The specific surface area, density, and porosity values for samples DAB1 and DAB2 are shown in Table 5.

Table 4. Atterberg limits of DAB1 and DAB2.

	Liquidity limit W_L (%)	Plasticity limit W_P (%)	Plasticity index I_P	Consistency index I_C
DAB1	72	35	37	1.88
DAB2	58	28	30	1.99

Table 5. Specific surfaces, densities and porosities of samples DAB1 and DAB2.

Samples	DAB1	DAB2
Specific surface ($m^2\ g^{-1}$)	39.16	25.72
Apparent density ($g\ cm^{-3}$)	2.47	2.72
Porosities (%)	60	54

4. Discussion

The high silica and alumina contents indicate that these two samples are aluminosilicates [33]. The Al_2O_3 percentage in samples DAB1 (21.87%) and DAB2 (28.11%) is low compared with pure kaolinite (37.30% and 40.46%) [34]. The Fe_2O_3 iron oxide content is relatively high. This high content suggests the existence of both structural and non-structural iron in the samples [35]. Literature sources [25] [26] show that iron exists in soils as oxides and oxy-hydroxides. The most important forms are Hematite (α-Fe_2O_3), Maghemite (γ-Fe_2O_3), Goethite (α-FeOOH), Lepidocrocite (γ-FeOOH) and Ferrihydrite (Fe_2O_3, xH_2O with $0.5 < x < 2.5$). Sample DAB2 contains around 11.55% Fe_2O_3. We can describe it as a lateritic clay. [36] states that a lateritic clay contains between 10% and 50% Fe_2O_3. [37] suggests that high iron content may induce hydroxyl radical production via the Fenton reaction. Iron in natural clays exists in various forms. It appears in the octahedral or tetrahedral layer. It can be adsorbed on the platelet surface or weakly intercalated in the interplatelet space. Iron converts reversibly from Fe^{II} to Fe^{III} in the octahedral layer of clays [38]. These redox reactions are particularly useful in Fenton-type degradation reactions [39]. The iron content in sample DAB1 (9.16%) according to EDS is high. This sample can therefore serve as a heterogeneous Fenton catalyst. Its iron content exceeds that of montmorillonite K10 (8.48%). [40] used this material to decolorize 99% of a 50 mg L^{-1} dye solution (Acid red 1). The porosity values of the samples are virtually identical. The densities of these clays range between 2.4 and 2.8 g cm^{-3}. This agrees with clay raw material values that generally fall within this range [41]. These results confirm the predominance of clay minerals in these different clay samples. The highest value (2.8 g cm^{-3}) measured for sample DAB2 agrees with that measured in laterites. Laterite values lie between 2.5 - 3.7 g cm^{-3} [42]. Atterberg limits characterize the consistency and plasticity of fine soils. The liquid limit WL values are 72% for DAB1 and 58% for DAB2. Sample DAB1 absorbs more water than sample DAB2. This correlates with the < 2 µm fraction and shows that DAB1 contains more consistent fine particles compared to DAB2. These trends confirm the granulometry results. Sample DAB1

contains more fine particles than sample DAB2. The plasticity index values (37 and 30, respectively, for DAB1 and DAB2) show that both samples are plastic because $20 < I_P < 40$ [32]. We conclude that DAB1 and DAB2 are plastic clays. The average consistency index (Ic average) of 1.93 exceeds 1. This shows that the samples are in a state of hard consistency. This makes them suitable for use in structural ceramics.

5. Conclusion

This study offers an in-depth analysis of two clay samples from Youhouil, Dabou, combining mineralogical, chemical, and geotechnical methodologies. ICP-AES results identified main oxides—SiO_2, Al_2O_3, and Fe_2O_3—with DAB1 comprising 67.54% SiO_2 and DAB2 58.21%. XRD analysis confirmed that both samples are predominantly kaolinite (51.12% and 65.75%), alongside quartz impurities (~35% - 42%). Particle size distribution showed that DAB1 has a higher clay content (73.5%) and finer particles, corroborated by D10, D50, and D90 values. The plasticity indices (37 for DAB1 and 30 for DAB2) indicate that both samples are highly plastic. Chemical mapping revealed a uniform distribution of aluminum and oxygen, with localized zones rich in carbon, silicon, iron, and titanium. Although potassium and sodium were not detected via EDS, their oxide forms were present at low concentrations according to ICP-AES. These features suggest that both clays have promising applications, notably in removing dye-related micropollutants from water through the heterogeneous Fenton process, where they could replace traditional iron-support materials. The results highlight the potential for valorizing native clays in industrial sectors such as ceramics and water treatment, supporting regional socioeconomic development. Further analytical work, including EPR and Mössbauer spectroscopy, is recommended to clarify the oxidation states and specific iron species involved in such processes.

Conflicts of Interest

The authors declare no conflicts of interest regarding the publication of this paper.

References

[1] Andji, Y.Y.J., Sei, J., Abba, T.A., Kra, G. and Njopwouo, D. (2001) Caractérisation min ralogique de quelques échantillons d'argile du site de GOUNIOUBE (Côte d'Ivoire). *Le Journal de la Société Ouest-Africaine de Chimie*, **11**, 143-166.

[2] Das, B.M. (2019) Principles of Geotechnical Engineering. 9th Edition, Cengage Learning.

[3] Yao, S. and Kouadio, K.B. (2020) Climatic and Geological Influences on the Geotechnical Properties of Tropical Soils. *Journal of Geotechnical and Geoenvironmental Engineering*, **146**, Article 04020011.

[4] Mbonu, C.C., Nwankwo, I. and Eze, C. (2021) Influence of Climatic Factors on the Geotechnical Properties of Tropical Soils. *Geotechnical and Geological Engineering*, **39**, 2215-2228.

[5] ASTM D4318-17 (2017) Standard Test Methods for Liquid Limit, Plastic Limit, and Plas-

ticity Index of Soils. ASTM International.

[6] Osei, K., Boateng, K. and Agyekum, K. (2022) Assessment of Regional Soils for Infrastructure Projects in West Africa. *Journal of African Earth Sciences*, **180**, Article 104224.

[7] Association Française de Normalisation (1996) Analyse granulométrique-méthode de tamisage à sec après lavage, NF P. 94-056.

[8] Association Française de Normalisation (1992) Analyse granulométrique dessols-méthode par sédimentation, NF P. 94-057.

[9] Association Française de Normalisation (1993) Détermination des limites d'Atterberg—Limite de liquidité à la coupelle—Limite de plasticité au rouleau, NF P. 94-051.

[10] Atsé, W.A., Essi, M.M.M., Doubi, B.I.H.G., Kamagaté, M., Aké, A.P. and Kouamé, A.N. (2022) Physico-Chemical Characterization of Two Dabou Clays with a View to Use Them in the Treatment of Dyeing Wastewater. *Journal of Minerals and Materials Characterization and Engineering*, **10**, 505-517. https://doi.org/10.4236/jmmce.2022.106036

[11] Smith, A.R., Johnson, P.M. and Patel, R. (2021). Advances in Low-Temperature Drying Techniques for Environmentally Friendly Ceramic Processing. *Chemical Engineering Journal*, **425**, Article 131359.

[12] Lee, S., Kim, J. and Choi, H. (2020) Effects of Particle Size and Morphology on the Drying Kinetics of Ceramic Powders. *Powder Technology*, **369**, 106-116.

[13] Chen, X., Liu, Y. and Zhou, G. (2019) Impact of Raw Material Characteristics on the Drying Behavior of Clay-Based Composites. *Journal of Sustainable Materials and Technologies*, **22**, e00100.

[14] Rosellyne S.D. (2021) Development of Silicate Ceramics from Clay-Based Raw Materials and a Vegetal Waste from Central Africa: Physicochemical Characteristics and Sintering. PhD Thesis, University of Limoges and the University of Lomé.

[15] Ngoro-Elenga, F., Ngopoh, A.I., Elenga, H., Mambou, J., Ngolo, J.N.N. and Nsongo, T. (2021) Characterization and Application of the Makoua Clay in the Chemical and Bacteriological Depollution of Gutter and Well Waters of Brazzaville. *Materials Sciences and Applications*, **12**, 263-275. https://doi.org/10.4236/msa.2021.126018

[16] Kouakou, L.P.M.-S., Kouamé, A.N., Doubi, B.I.H.G., Méité, N., Kangah, J.T., Zokou, E.P., *et al.* (2022) Characterization of Two Clay Raw Materials from Côte d'Ivoire with a View to Enhancing Them in Eco-Construction. *Journal of Minerals and Materials Characterization and Engineering*, **10**, 198-208. https://doi.org/10.4236/jmmce.2022.102016

[17] Kouamé, A.N., Konan, L.K., Doubi Gouré, B.I.H.G., Tognonvi, M.T. and Oyetola, S. (2020) Mechanical and Microstructural Properties of Compressed Earth Bricks (CEB) Incorporating Shea Butter Wastes and Stabilized with Cement. *Journal of Materials Physics and Chemistry*, **8**, 1-8.

[18] Laibi, A.B., Gomina, M., Sorgho, B., Sagbo, E., Blanchart, P., Boutouil, M., *et al.* (2017) Caractérisation physico-chimique et géotechnique de deux sites argileux du Bénin en vue de leur valorisation dans l'éco-construction. *International Journal of Biological and Chemical Sciences*, **11**, 499-514. https://doi.org/10.4314/ijbcs.v11i1.40

[19] Méité, N., Kouakou, L.P.M., Kouamé, A.N., Pohan, A.G.L., Sanou, I., Cissé, G., *et al.* (2024) Study of the Influence of Clay in the Degradation of Methylene Blue by Photo-Fenton Process. *Materials Sciences and Applications*, **15**, 538-557. https://doi.org/10.4236/msa.2024.1511036

[20] Kouadio, L.M., Lebouachera, S.E.I., Blanc, S., Sei, J., Miqueu, C., Pannier, F., *et al.*

(2022) Characterization of Clay Materials from Ivory Coast for Their Use as Adsorbents for Wastewater Treatment. *Journal of Minerals and Materials Characterization and Engineering*, **10**, 319-337. https://doi.org/10.4236/jmmce.2022.104023

[21] Pierre, A.A., Brice, K.A. and Vamoussa, C. (2021) Kinetic and Thermodynamic Study of the Dephosphation of Wastewater by Clay Materials from Côte d'Ivoire. *Open Journal of Applied Sciences*, **11**, 1307-1323. https://doi.org/10.4236/ojapps.2021.1112099

[22] Kpinsoton, G.M.R., Karoui, H., Richardson, Y., Koffi, B.N.S., Yacouba, H., Motuzas, J., *et al.* (2018) New Insight into the Microstructure of Natural Calcined Laterites and Their Performance as Heterogeneous Fenton Catalyst for Methylene Blue Degradation. *Reaction Kinetics, Mechanisms and Catalysis*, **124**, 931-956. https://doi.org/10.1007/s11144-018-1406-0

[23] Kamagate, M., Amin Assadi, A., Kone, T., Coulibaly, L. and Hanna, K. (2018) Activation of Persulfate by Irradiated Laterite for Removal of Fluoroquinolones in Multi-Component Systems. *Journal of Hazardous Materials*, **346**, 159-166. https://doi.org/10.1016/j.jhazmat.2017.12.011

[24] Garcia-Valles, M., Alfonso, P., Martínez, S. and Roca, N. (2020) Mineralogical and Thermal Characterization of Kaolinitic Clays from Terra Alta (Catalonia, Spain). *Minerals*, **10**, Article 142. https://doi.org/10.3390/min10020142

[25] Sei, J., Jumas, J.C., Olivier-Fourcade, J., Quiquampoix, H. and Staunton, S. (2002) Role of Iron Oxides in the Phosphate Adsorption Properties of Kaolinites from the Ivory Coast. *Clays and Clay Minerals*, **50**, 217-222. https://doi.org/10.1346/000986002760832810

[26] Soro N.S. (2003) Influence des ions fer sur les transformations thermiques de la kaolinite. Thèse de Doctorat de l'Université de Limoges.

[27] Benjelloun, Y., Miyah, Y., Idrissi, M., Boumchita, S., Lahrichi, A. and Lalami, A.E.O. (2016) Étude de la Performance Catalytique Pendant l'Oxydation du Bleu de Méthylène en Utilisant un Catalyseur MnO-Argile en Présence de H_2O_2. *Journal of Materials and Environmental Science*, **7**, 9-17.

[28] Guerraoui, F., Zamama, M. and Ibnoussina, M. (2009) Thermal Behaviour of the Ceramic and Pottery of Safi-Morocco. *Physical and Chemical News*, **49**, 114-120.

[29] He, I.L., Atheba, G.P., Allou, N.B., Drogui, P., EI Khakani, M.A. and Gbassi, G.K. (2023) Physic, Chemical and Mineralogical Characterizations of Clays Used in the Making of Traditional Ceramics in the City of Katiola, Côte d'Ivoire. *Journal of Minerals and Materials Characterization and Engineering*, **11**, 81-91. https://doi.org/10.4236/jmmce.2023.114008

[30] Guyot, J. (1969) Mesure des surfaces spécifiques des argiles par adsorption. *Annales agronomiques*, **20**, 333-359.

[31] Jozja, N. (2003) Etude de matériaux argileux albanais: Caractérisation multi-échelle d'une bentonite magnésienne: Impact de l'interaction avec le nitrate de plomb sur la perméabilité. Thèse de doctorat, Université d'Orléans.

[32] Wetshondo Osomba, D. (2012) Caractérisation et valorisation des matériaux argileux de la Province de Kinshasa (RD Congo). Thèse de doctorat, Université de Liège.

[33] Nirmala, G. and Viruthagiri, G. (2015) A View of Microstructure with Technological Behavior of Waste Incorporated Ceramic Bricks. *Spectrochimica Acta Part A: Molecular and Biomolecular Spectroscopy*, **135**, 76-80. https://doi.org/10.1016/j.saa.2014.06.150

[34] Amareli. P. (2005) Nanocomposites polyméthacrylate de méthyle-silicates lamellaires. Influence de la nature de la charge et de de l'interface sur les propriétés mécaniques

et sur la transition vitreuse, Université Pierre et Marie Curie–Paris VI.

[35] Coulibaly, V. (2013) Contribution à l'étude des argiles consommées en Côte d'Ivoire: Minéralogie, Réactivité dans les conditions digestives, Radioactivités. Thèse de Doctorat d'Etat ès Sciences Physiques de l'Université Félix Houphouët Boigny (UFHB), Abidjan, Côte d'Ivoire.

[36] Lacroix, A. (1913) Les latérites de la Guinée et les produits d'altération qui leur sont associés. Masson et cie.

[37] Williams, L.B., Haydel, S.E., Giese, R.F. and Eberl, D.D. (2008) Chemical and Mineralogical Characteristics of French Green Clays Used for Healing. *Clays and Clay Minerals*, **56**, 437-452. https://doi.org/10.1346/ccmn.2008.0560405

[38] Stucki, J., Bailey, G. and Gan, H. (1995) Redox Reactions in Phyllosilicates and Their Effects on Metal Transport. In: Allen, H.E., Huang, C.P., Bailey, G.W. and Bowers, A.R., Eds., *Metal Speciation and Contamination of Soil*, Lewis Publishers, 113-181.

[39] De León, M.A., Castiglioni, J., Bussi, J. and Sergio, M. (2008) Catalytic Activity of an Iron-Pillared Montmorillonitic Clay Mineral in Heterogeneous Photo-Fenton Process. *Catalysis Today*, **133**, 600-605. https://doi.org/10.1016/j.cattod.2007.12.130

[40] Daud, N.K., Ahmad, M.A. and Hameed, B.H. (2010) Decolorization of Acid Red 1 Dye Solution by Fenton-Like Process Using Fe-Montmorillonite K10 Catalyst. *Chemical Engineering Journal*, **165**, 111-116. https://doi.org/10.1016/j.cej.2010.08.072

[41] Lamloumi, R. (2015) Comportement des matériaux minéraux de grande diffusion lors du séchage. Thèse de doctorat en cotutelle, Université de Limoges.

[42] Maignien, R. (1958) Le cuirassement des sols en Guinée, Afrique Occidentale [The Cuirassement of Soil in Guinea, West Africa]. Thèse Sciences Université de Lorraine Strasbourg, 239.